THE NEGATIVE TRANSMISSIBILITY ISSUE WHEN USING CVFEM IN PETROLEUM RESERVOIR SIMULATION – 2. RESULTS

Jonas Cordazzo
jonas@sinmec.ufsc.br

Clovis R. Maliska
maliska@sinmec.ufsc.br

Antonio F. C. da Silva
fabio@emc.ufsc.br

Fernando S. V. Hurtado
fernando@sinmec.ufsc.br

Federal University of Santa Catarina – UFSC
Computational Fluid Dynamics Laboratory – SINMEC – **www.sinmec.ufsc.br**
Department of Mechanical Engineering, 88040-900, Florianopolis, Santa Catarina, Brazil

Abstract: This paper presents a comparison among the results obtained by the Control Volume Finite Element Method (CVFEM) in the form it is presented in the reservoir simulation literature, called here CVFEM-S, and the one that resembles the traditional CVFEM used in fluid mechanics and heat transfer, called here CVFEM-M. Details of these methods were described and discussed in a companion paper, and the basic difference between them is that the CVFEM-S equations for multiphase flow in petroleum reservoir simulation are derived based on a single-phase flow, and then extended to multiphase formulations by the addition of the mobility term, whereas the CVFEM-M uses the multiphase flow equations to derive the discretized equations. It is shown that in practical cases involving negative transmissibilities, the results of CVFEM-M are physically consistent whereas the CVFEM-S presents even negative saturations depending on the mobility scheme evaluation. For radial problems, the saturation distribution obtained by CVFEM-S was asymmetrical, whereas the CVFEM-M results presents the required symmetry. Finally, it is shown that the CVFEM-S is more susceptible to the grid orientation effect with the mobility ratio (M) increasing. The results permit to conclude that the assumptions of the CVFEM-S of starting from a single-phase formulation ends up in a scheme that has serious limitations for practical use.

Keywords: reservoir simulation, petroleum, control-volume, finite volume method, finite element method, transmissibility.

1. Introduction

This paper compares the numerical solutions obtained by the Control Volume Finite Element Method (CVFEM) as it is commonly presented in the reservoir simulation literature, called here CVFEM-S, with the one that resembles the traditional CVFEM used in fluid mechanics and heat transfer, called here CVFEM-M. In the petroleum reservoir literature, the discretized multiphase equations are deduced starting from the discretized equations of single-phase case. It is show that, if the mass-conservation differential equations were integrated considering the existence of more than one phase, the resulting discretized equations will be different. This procedure, which results in the CVFEM-M equations, is presented in a companion paper (Cordazzo et al., 2004).

The concept of transmissibility in structured and unstructured grids, using triangular and quadrilateral elements, is another important issue that was already discussed in Cordazzo et al., 2004). It was shown that a physical meaning for the transmissibility only exists when the flux in the volume interfaces is calculated using only two grid-points values, even in non-orthogonal grids. Nevertheless, the transmissibility is, in a number of situations, used in a misleading way, since the flux is calculated using three or more grid-points values. In this work, it is shown that when triangles disobeying the angular restriction precluded in the literature are used, the negative coefficients resulting from the discretization do actually have physical support, once they are not, in fact, "transmissibilities", as they are often referred in the literature.

Three different forms of mobility evaluating in triangular elements, as well as their impact on the results, are presented. At last, the grid orientation effect in simulations obtained by means of CVFEM-S and CVFEM-M is also discussed.

The solutions of the CVFEM-S were obtained by two different ways in this work: one of them solving the discretized equations using C++ (in-house software), and other one using the commercial simulator STARS of CMG, with the option CVFE (Stars User's Guide, 2002). These two results always agreed in all cases analyzed. For the

CVFEV-M, results were obtained only by solving its discretized equations using another in-house software, also implemented in C, since there is no commercial, or other application, which employs this approach.

2. Comparison between the CVFEM-M and CVFEM-S results

In this section, five test problems are studied with the purpose of comparing the results of the two different conservative methods addressed in this work, both dealing with triangular grids.

Problem 1. **Interpretation of the negative "transmissibilities" coefficients in triangular grids**

For this study, the homogeneous and isotropic porous media shown in Fig. 1 is considered, where 5 wells, 2 injectors (nodes 3 and 5) and 3 producers (nodes 1, 2 and 4), with the same block pressure prescribed. Water and oil viscosities are identical and the flow is incompressible. The arrangement of wells and grid-elements was chosen in order to induce a parallel flow in the *x* direction inside each element, since the pressures in the nodes 3 and 5 will result the same.
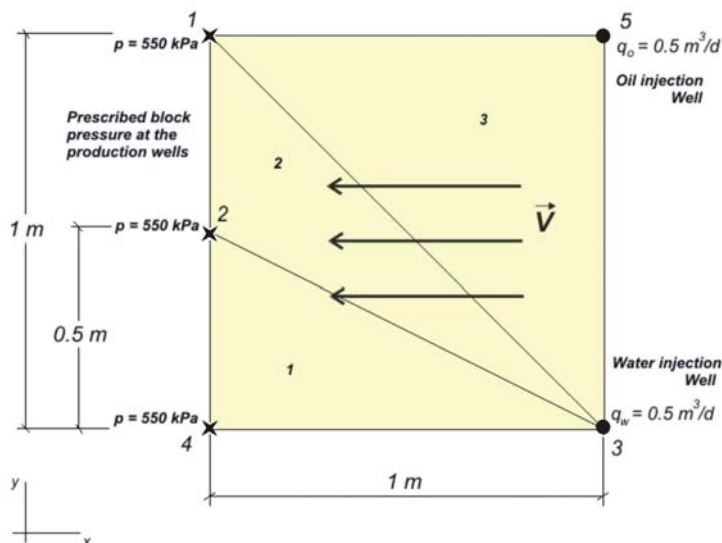
Figure 1 – Domain of Problem 1

The element under analysis in this example is the element 123 (denoted by the number 2) for having an internal angle greater than 90°. According to some authors, elements with these characteristics should be avoided because they would origin negative transmissibilities (Fung et al*.,* 1993; Sonier et al., 1993). In Fig. 2 this element and its respective sub-control volumes are shown. The choice of locating the point *B*, in turn, is arbitrary, but often the barycenter of the triangle is chosen. There are at least two reasons that can justify this choice: *(1)* the triangles are always divided in 3 sub-control volumes with the same area, and *(2)* it is easy to build a general procedure for computational implementation in the local coordinates. This procedure allows each element to be treated identically, no matter how distorted the element may actually be in terms of the global coordinates. Though, other positions of the central point *B* inside the triangle yields identical conclusions as the ones obtained in this paper (Palagi, 1992).
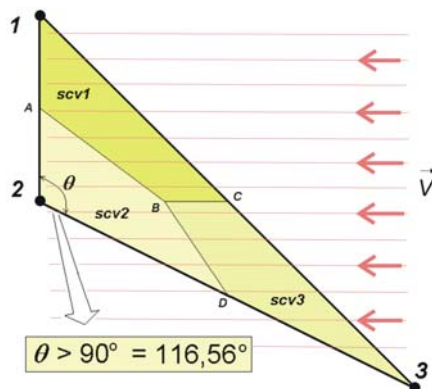
Figure 2 – Triangular element 2 of Fig. 1, showing its sub-control volumes and the velocity field

According to Fig. 1, the pressures at the production wells 1 and 2 are identical ($p_2 = p_1$), moreover $p_3 > p_1$ since a injection well is located at the node 3, hence the mass flow-rate equation deduced in the previous paper (Cordazzo et al., 2004), written for the sub-control volume 1, *scv1*, in Fig. 2, yields

$$Q_1 = Q_{AB} + Q_{BC} = \Im_{13_{Svc1}}(p_3 - p_1) + \Im_{12_{Svc1}}(p_2 - p_1)$$

$= 0$ (because $p_2 = p_{1.}$)

resulting in

$$Q_1 = \Im_{13_{Svc1}}(p_3 - p_1) \tag{1}$$

where $\Im_{13_{Svc1}}$ is another term deduced also in the previous paper, given by

$$\Im_{13_{Svc1}} = \lambda_{12}\tau^{13}_{AB_{Svc1}} + \lambda_{13}\tau^{13}_{BC_{Svc1}}$$

$= 0$ (because $\vec{V}.\Delta\vec{S}_{BC} = 0$, since the segment *BC* is located parallel to the flow)

Thus, the total mass flow-rate through the inner interface of the sub-control volume 1 in Fig. 2 is given by

$$Q_1 = \lambda_{12}\tau^{13}_{AB_{Svc1}}(p_3 - p_1) \tag{2}$$

By inspection of Figs. 1 and 2, it is easy to conclude that the flow-rate given by Eq. 2 is the one that "goes" only through the segment *AB*, since the segment *BC* is located parallel to the flow, as already stated. Note also that there is no relation with the sub-control volume 3, as it could be suggested for the presence of the term ($p_3 – p_1$) in Eq. 2, because the fluid actually "goes" from *Scv1* to *Scv2*. This observation has not yet been clarified in the literature, although Palagi (1992) has given important contributions in this direction in the appendix of his thesis.

Analyzing physically Fig. 2, one can see that the flow is "going" from sub-control volume 1 to the sub-control volume 2, as mentioned before, hence the flux Q_1 must have a negative signal

$$Q_1 = \lambda_{12}\tau^{13}_{AB_{Svc1}}(p_3 - p_1) < 0$$

and as the mobility is always a positive value by definition, and the term ($p_3 – p_1$) > 0 in this case, we conclude that

$$\boxed{\tau^{13}_{AB_{Svc1}} < 0}$$

which is, therefore, physically correct, even though it cannot be called transmissibility if its correct physical interpretation is considered (Cordazzo et al., 2004). Perhaps the presence of these negative coefficients could imply some difficulty on the convergence of linear solvers, but from a physical or a numerical point of view there is not any incoherence with the signal of these coefficients. The key question is that this coefficient is usually called transmissibility in the literature, and since it is negative, it is recommended not to use such a distorted triangle, because transmissibility can not be negative. In fact, there is nothing wrong with that, since this value is merely a negative coefficient.

Problem 2: **Mobility evaluation issue and comparison of CVFEM-S and CVFEM-M results**

Another study involving the grid of Fig. 2 was carried out with the results obtained using CVFEM-S and CVFEM-M. First of all, one needs to consider the mobility evaluation at the control-volume interfaces in both methods. According to the scheme used, the results may become very different. Although several schemes could be devised, three alternatives are analyzed here.

Firstly, the scheme used in the CVFEM-S initially consisted of evaluating the mobilities by the usual finite difference approach (Fung et al., 1991), called here scheme 1, where the upstream weighting is given by

$$\lambda_{ij} = \lambda_i \qquad \text{if} \qquad p_i > p_j \tag{3a}$$

$$\lambda_{ij} = \lambda_j \qquad \text{if} \qquad p_j > p_i \tag{3b}$$

As several difficulties are verified when this scheme is used with triangles that "violate" the angular restriction, as we will see further, Fung et al. (1993) proposed a little modification in Eq. 3, such that the coefficient (inappropriately called "transmissibitiy)" T_{ij} could be considered in this expression (scheme 2):

$$\lambda_{ij} = \lambda_i \qquad \text{if} \qquad T_{ij}(p_i - p_j) > 0 \qquad\qquad (4a)$$

$$\lambda_{ij} = \lambda_j \qquad \text{if} \qquad T_{ij}(p_i - p_j) < 0 \qquad\qquad (4b)$$

As scheme 3, it is proposed here ,for the CVFEM-M, to determine the interfaces mobility values by evaluating the signal of the following scalar products

$$\lambda_{ij} = \lambda_i \qquad \text{if} \qquad \left(\overline{\overline{k}}\vec{\nabla}p\right).\hat{n}_{ij} \leq 0 \qquad\qquad (5a)$$

$$\lambda_{ij} = \lambda_j \qquad \text{if} \qquad \left(\overline{\overline{k}}\vec{\nabla}p\right).\hat{n}_{ij} > 0 \qquad\qquad (5b)$$

where $\hat{n}_{ij}$ is the normal vector to the interface between the sub-volumes *i* and *j,* being outgoing normal to the face of volume *i*. Note that this scheme is based on the evaluation of the flow direction, even though the mobility term was omitted in Eq. 5, because it yields always a positive value. The scheme presented in Eq. 5 assures that the mobilities evaluated at the interfaces are the ones located on the upstream direction, even in cases where the media is anisotropic, i. e. when the velocity vector is not aligned with the potential gradient.

The calculation of the mass flow-rate Q_1, which is leaving sub-control volume 1 according to Figs. 1 and 2, employing the three previous mobility evaluation schemes, is now analyzed. Consider, for instance, that the water saturation in each of the nodes in Fig. 2 is set as

$$Sw_1 = 0 \qquad\qquad Sw_2 = 0 \qquad\qquad Sw_3 = 1$$

Beginning with the CVFEM-M, the mass flow-rate Q_1 deduced by this method is given by Eq. 2. We can see by inspection of Figs. 1 and 2, and according to Eq. 5 (scheme 3), that the upstream saturation value used for determining the water mobility λ_{12_w} is zero (since $Sw_1 = Sw_2 = 0$). Thus,

$$\boxed{Q_{1_w} = 0}$$

as expected, since the volume 1 has no water, and the flux goes from right to left, i. e. from volume 1 to volume 2 in the segment *AB*. This agrees with the physics of the problem being studied.

In the CVFEM-S, however, the mass flow-rate Q_1 is given by (Fung et al., 1991):

$$Q_1 = \lambda_{13}T_{13}(p_3 - p_1) + \lambda_{12}T_{12}(p_2 - p_1) \qquad\qquad (6)$$

Due to data used in this problem ($Sw_1 = Sw_2 = 0$) we have already seen that the mobility λ_{12_w} must be zero, so Eq. 6, written for water, is reduced to

$$Q_{1_w} = \lambda_{13_w}T_{13}(p_3 - p_1) \qquad\qquad (7)$$

where T_{13} is a coefficient deduced in the previous paper. Using the geometrical information of the grid in Fig. 1, this coefficient can be calculated, and in this case it is given by

$$T_{13} = -0,25k$$

and substituting it into Eq. 7 yields

$$Q_{1_w} = -0,25\lambda_{13_w}k(p_3 - p_1) \qquad\qquad (8)$$

The choice of the mobility evaluation scheme is now even more decisive. For instance, if the option is to utilize the scheme 1, Eq. 3, the mobility λ_{13_w} will be calculated with the saturation of node 3, becoming the product $\lambda_{13_w}k(p_3 - p_1)$ positive for this problem, in a way that the water flux will be

4

$Q_{1_w} < 0$

> Hence,
> there would be water flowing OUT of a
> volume which has no water!

To avoid this type of difficulties when utilizing the CVFEM-S, one can use the scheme 2 defined by Eq. 4. So, for the case studied here, the mobility λ_{13w} will be calculated, instead of using the saturation of node 3, using the saturation of node 1, which is zero. This yield

$Q_{1_w} = 0$

which is physically consistent. But, the term $T_{ij}\left(p_i - p_j\right)$ is not actually the mass flow-rate between the volumes i and j, as could be suggested by this expression (Cordazzo et al., 2004). In addition, by inspection of Eq. 8, we can note that for any other case where the water saturation of node 1 is not zero, the mobility λ_{13w} will not be zero, resulting in a negative mass flow-rate, as happened using scheme 1.

The changing of the signal of fluxes that can occur in the CVFEM-S results only when obtuse triangles are used, being this the reason why some authors have recommended avoiding these elements. When only triangles having angles less the 90º are used, all fluxes have the correct sign, even though they are, probably, not correctly calculated in most cases. Obeying this angular restriction we can assure that the results remain physically reasonable. However, this is not necessary, since it limits considerably the flexibility of the grid system.

In order to compare the results of CVFEM-S and CVFEM-M for the problem depicted in Fig. 1, we use the following data: absolute permeability k = 150 mD, water and oil viscosities μ = 1 cp, porosity ϕ = 0.2, linear relative permeability curves and time step Δt = 0.001 day. The IMPES scheme was used in all cases in this work to solve the coupled non-linear resulting equations.

(a)

(b)

(c)
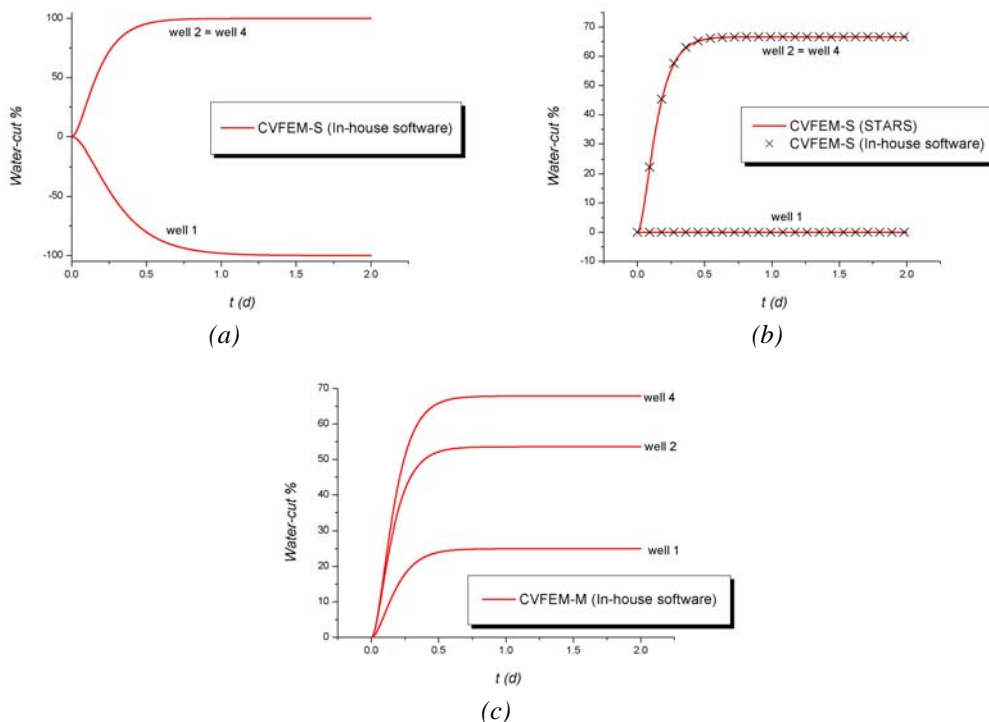
Figure 3 – Water-cut at the production wells vs. time for the porous media of Fig. 1 obtained by the methods: *(a)* CVFEM-S with mobility calculated by Eq. 3, *(b)* CVFEM-S with Eq. 4, and *(c)* CVFEM-M with Eq. 5

Figure 3 depicts the results obtained by two different methods (CVFEM-S and CVFEM-M) using three different schemes of evaluating the mobility (schemes 1 to 3) in terms of water-cut. The CVFEM-S with the scheme 1 produces the water-cut curves at the production wells 1, 2 and 4 depicted in Fig. 3a. The negative saturation values of well 1, and in consequence the negative production at this well, are caused by the use of the scheme of evaluating mobilities given by Eq. 3. The same method, however, which evaluates the mobilities by Eq. 4 no longer predict negative saturations, as shown in Fig. 3b. We can note that the match of the results obtained by the in-house software with the results of the commercial simulator STARS is very good, as should be. Figure 3c, on the other hand, depicts the results of CVFEM-

M with the mobility evaluation scheme given by Eq. 5. These results, besides the ones shown in Fig. 3*b*, are quite coherent, even though the results of CVFEM-S have not produced any water at well 1.

The results of STARS were obtained setting the $P = 550$ kPa (bottom hole pressure), and with high value of well index ($WI = 1.10^{10}$), since there is no way to prescribe directly block pressure values in that software. In the in-house software, in contrast, it was not difficult to prescribe the block pressure because the flux equations were deduced for that case.

In the following test problems, the mobility evaluation will be given by Eq. 4 and 5, for the CVFEM-S and for the CVFEM-M, respectively.

Problem 3: **Radial displacement**

The case analyzed in this section has been used to evaluate the grid orientation effect, and it was proposed by Bajor and Cormack (1989) for quadrilaterals grids. The geometry consists of a constant radius locus of producers, centered on a single injector. Here, ¼ of this radial field geometry is discretized using a grid composed by triangular elements, such as the one depicted in Fig. 4, with an injection well surrounded by 15 production wells symmetrically located.
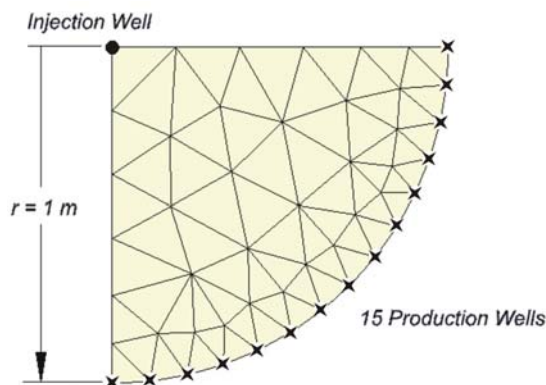
Figure 4 – Radial grid used to evaluate the grid orientation effect (48 nodes and 68 elements)

Table 1 – Reservoir fluids and rock data used for $M = 1$ in the radial problem

Porosity	0.2
Permeability (isotropic)	150 mD
Reservoir thickness	1 m
Viscosity of water	1 cP
Viscosity of oil	1 cP
Compressibility of water	0
Compressibility of oil	0
Volume formation factor of water	1
Volume formation factor of oil	1
Swi	0
kro@Swi	1
Sor	0
krw@Sor	1
Curve exponent (Corey) of krw	1
Curve exponent (Corey) of kro	1
Water flow-rate at the injection well	0.01 m³/d
Bottom-hole pressure at the production well	100 kPa
Well index	1 mD·m
Time step	0.01 d

The rock and fluid properties that are relevant to this problem, considering mobility ratio $M = 1$, are given in Tab. 1. The simulation with mobility ratio $M = 10$, on the other hand, will be also performed using the data in Tab. 1, but increasing the oil viscosity to 10 cp and replacing the relative permeability curves for:

$$k_{r_w} = \frac{s_w}{M(1 - s_w) + s_w} \qquad (9)$$

$$k_{r_o} = 1 - k_{r_w} \qquad (10)$$

Independently of the grid and the numerical method used, the water production should be identical at the wells, because of the problem symmetry. Figure 5 depicts the water production at the production wells versus time for different mobility ratios obtained by the different methods. As one can observe in this figure, the CVFEM-M results present small differences among the wells. Nevertheless, with the increasing of mobility, Fig. 5*b*, the results of CVFEM-M showed a little increase of the grid orientation effect. In the CVFEM-S results, this increase was more serious than the one obtained by the other method.

(a) $M = 1$

(b) $M = 10$
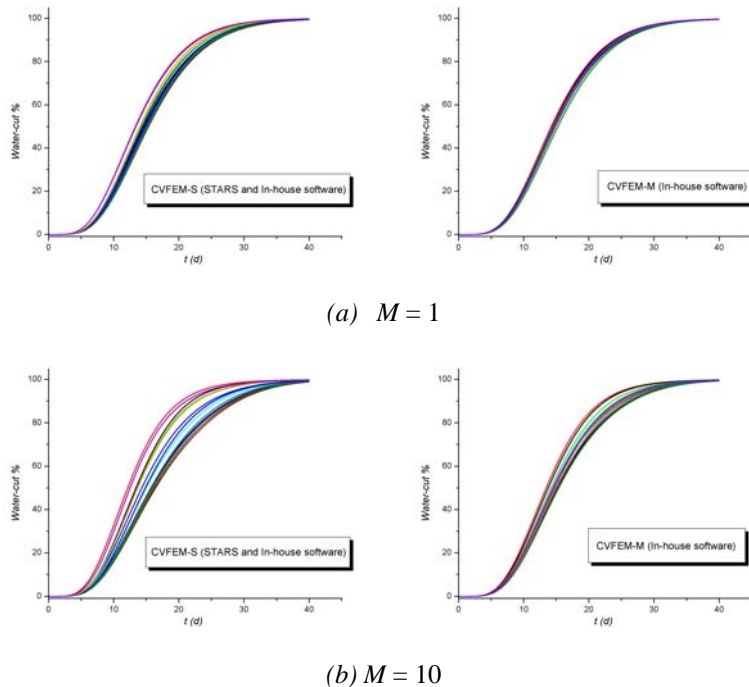
Figure 5– Water-cut at the production wells vs. time obtained by CVFEM-S and CVFEM-M for two different mobility ratios

Another way to show the differences presented in Fig. 5 is visualizing the water-saturation contour. In the case analyzed here, it is enough to consider the mobility ration $M = 1$, which results in the iso-lines of Fig. 6, for the simulation time 23.338 days. The iso-lines of the CVFEM-S, Fig. 6*a*, seem to be less symmetrical than the iso-lines of the CVFEM-M, Fig. 6*b*. The iso-saturation of 0.9 obtained by STARS is almost the same the one obtained by the in-house software, as we can see superimposed them in Fig. 6*a*.

(a)   *(b)*
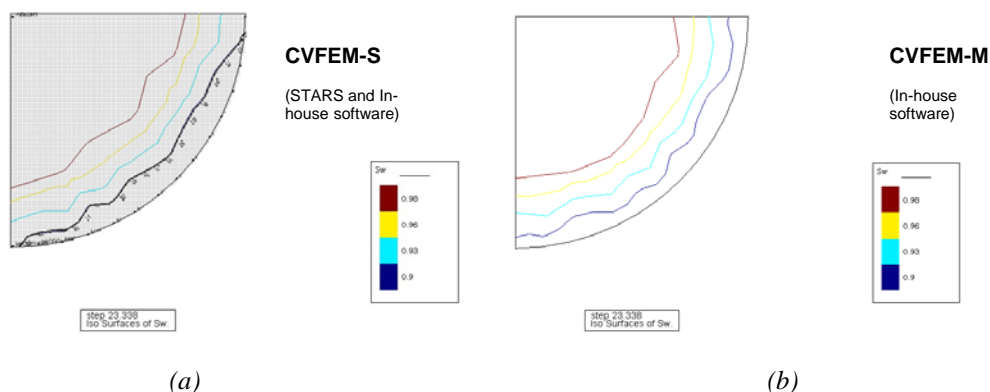
Figure 6 – Water-saturation contour at 23.338 days, obtained from: *(a)* CVFEM-S (STARS and in-house results are superimposed), and *(b)* CVFEM-M

Problem 4: **Five-Spot**

The *five-spot* is a well known arrangement used in order to study the grid orientation effects in numerical simulation, proposed by Todd et al. (1972). It consists of a repetitive pattern where each production well is surrounded by four injection wells. Due to its geometrical symmetry, it is usually discretized by two grids: a diagonal one and a parallel one, shown in Figs. 7*a* and 7*b*. The diagonal grid represents a quarter of a five-spot pattern, while the parallel

grid represents one-half of a five-spot pattern. This scheme allows showing easily the disparity in results for equivalent parallel and diagonal grids for adverse mobility ratio, mainly on Cartesian grids.

| *(a)* Diagonal grid | *(b)* Parallel grid | *(c)* Superimposition of the two grids |
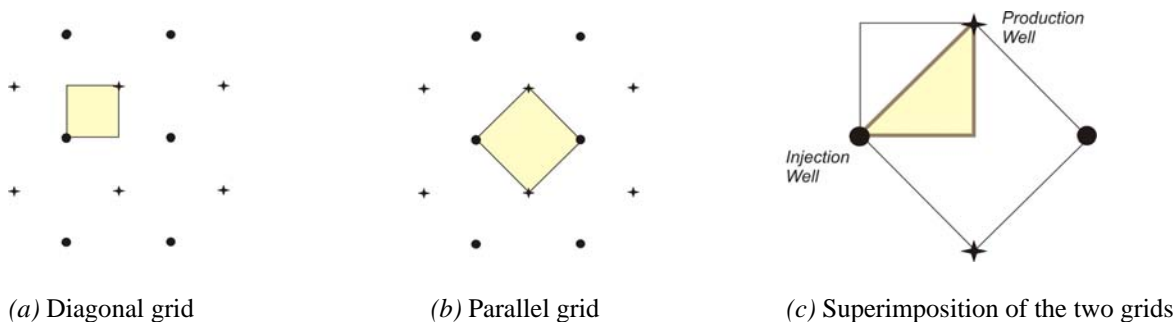
Figure 7 – Grids used in the five-spot pattern

Due to the using of triangular elements in the discretization of the domain, one can facilitate the interpretation of the results simulating the flow only in the triangular region depicted in Fig. 7*c*, using grids like the ones presented in Fig. 8, which represent, in a five-spot scheme, ¼ and ½ of a parallel grid and diagonal grid, respectively. Note that the triangles are rotated by 90° between the two figures.

| *(a)* Parallel grid | *(b)* Diagonal grid |
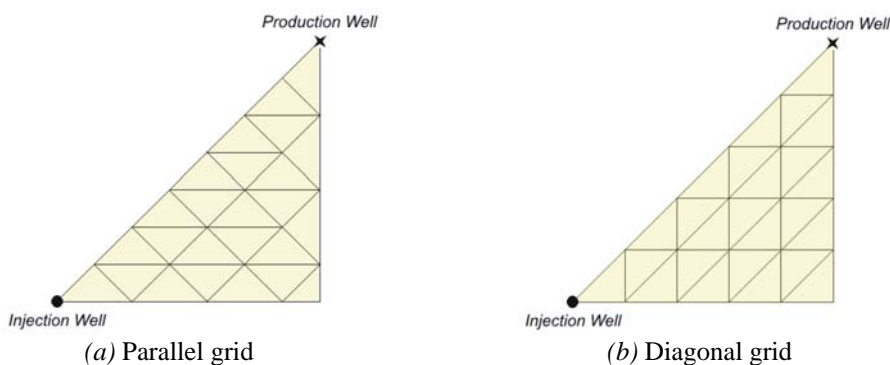
Figure 8 – Grids used in the five-spot problem (21 nodes and 25 elements)

Three cases were simulated involving three different mobility ratios: $M = 1$, 4 and 10. The data used in the simulation with $M = 1$ are presented in Tab. 2, while for other cases the oil viscosity was modified ($\mu_o = 4$ and 10 cp) as well as the relative permeability curves that were defined by Eqs. 9 and 10.

Table 2 – Reservoir fluids and rock data used for $M = 1$ in five-spot problem

Porosity	0.2
Permeability (isotropic)	150 mD
Reservoir thickness	1 m
Viscosity of water	1 cP
Viscosity of oil	1 cP
Compressibility of water	0
Compressibility of oil	0
Volume formation factor of water	1
Volume formation factor of oil	1
Swi	0
kro@Swi	1
Sor	0
krw@Sor	1
Curve exponent (Corey) of krw	1
Curve exponent (Corey) of kro	1
Water flow-rate at the injection well	0.05 m³/d
Bottom-hole pressure at the production well	100 kPa
Well index	1 mD.m
Time step	0.001 d

The results obtained by the CVFEM-M and the CVFEM-S for the grids shown in Fig. 8 are plotted in Fig. 9, for different mobility ratios *M*. We can note that although both methods have presented disparities between the results on the diagonal and parallel grids, in the CVFEM-S the grid orientation effects increase even more with the mobility ratio. In turn, the result for $M = 10$, Fig. 9c, was not possible to run with the software STARS. Thus the result obtained by the in-house software was the only shown using this mobility ratio. Curiously, however, for all mobility ratios studied, the diagonal grid results of the CVFEM-M are near to the parallel grid results of the CVFEM-S, implying in an opposed grid orientation effect on the CVFEM-M results.

The recovery behavior of the CVFEM-S depicted in Fig. 9 is almost identical to those of Cartesian grids (Yanosik and McCracken, 1979; Bajor and Cormack, 1989; Shin and Merchant, 1993). So, this is the reason why grids constructed by dividing quadrilaterals into right angle triangles has been prevented in the literature. Actually, this grid orientation effect happens in this kind of triangular grids because the coefficients between nodes opposite right angles are null in the CVFEM-S, resulting in a typical five-point scheme.

(a) M = 1   *(b) M = 4*

(c) M = 10
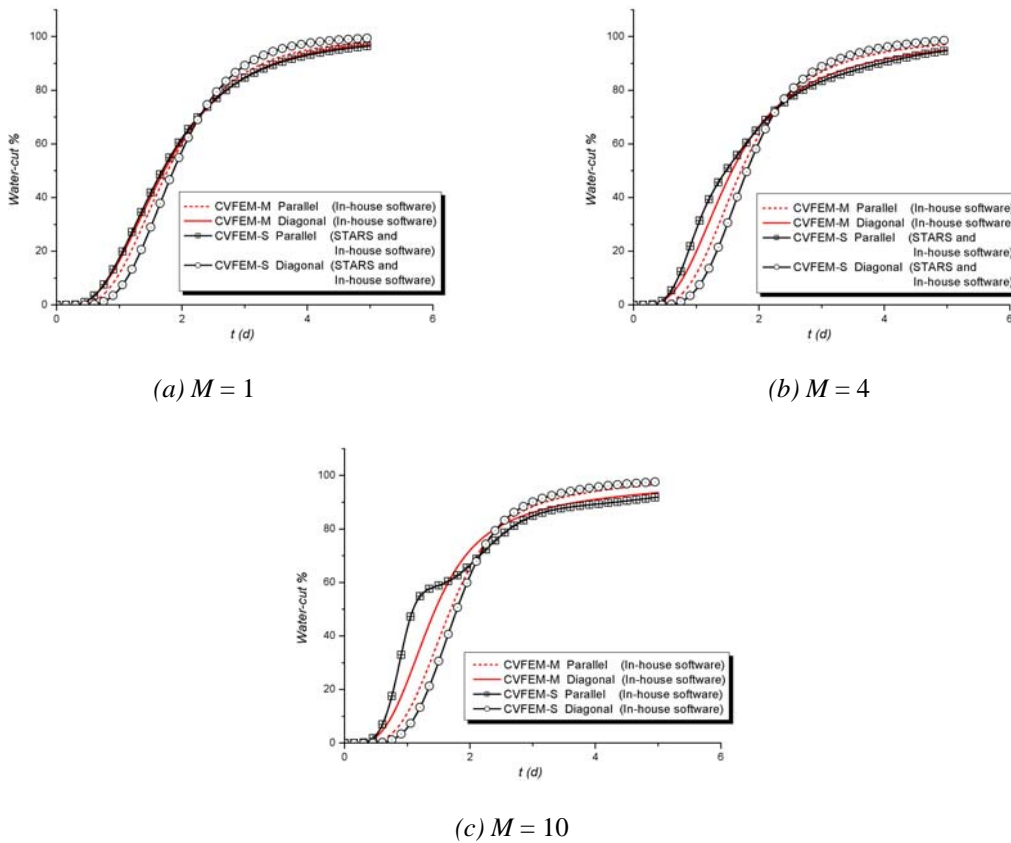
Figure 9 – Comparison of grid orientation effects between the CVFEM-M and CVFEM-S, utilizing the diagonal and parallel five-spot triangular grids, for different mobility ratios *M*

In Fig. 10 the grid orientation effects is also examined by comparing the water-saturation contours at 0.834 days, for the parallel and diagonal grids. The runs were performed with $M = 4$, using the CVFEM-S (by STARS and the in-house software) and the CVFEM-M (by the in-house software). Again, it is shown that the grid orientation effect on the CVFEM-M is less accentuated.

Parallel grid   Diagonal grid

(a) CVFEM-S (STARS and in-house results are superimposed)
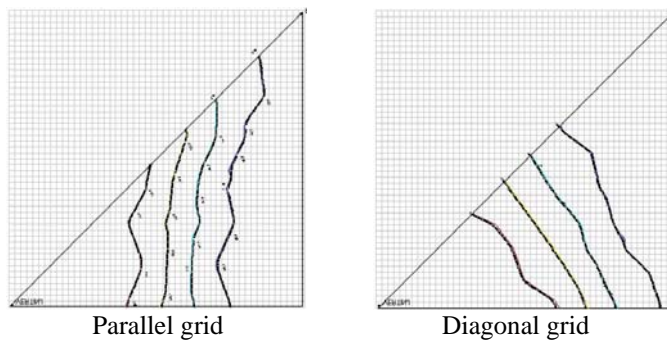
Parallel grid   Diagonal grid
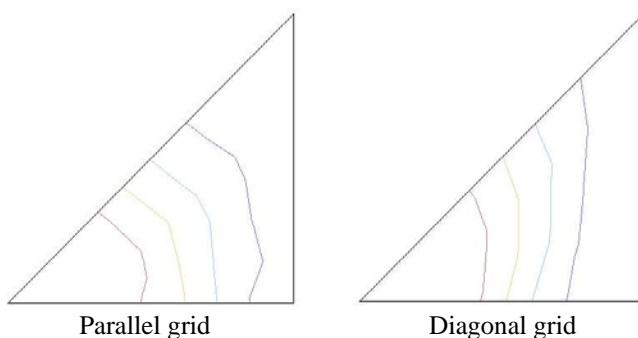
(b) CVFEM-M

Figure 10 – Predicted water iso-saturation ($S_w = 0.2, 0.4, 0.6$ and 0.8) for mobility ratio $M = 4$, at 0.834 days.

Problem 5: **Grid formed only by obtuse triangles**

The last case analyzed in this paper consists of a petroleum reservoir discretized using a grid composed only by obtuse triangular elements, i. e. triangles that have a angle greater than 90º, as depicted in Fig. 11. The water injection well is at the lower-right corner, whereas the production well is at the opposite diagonal corner.
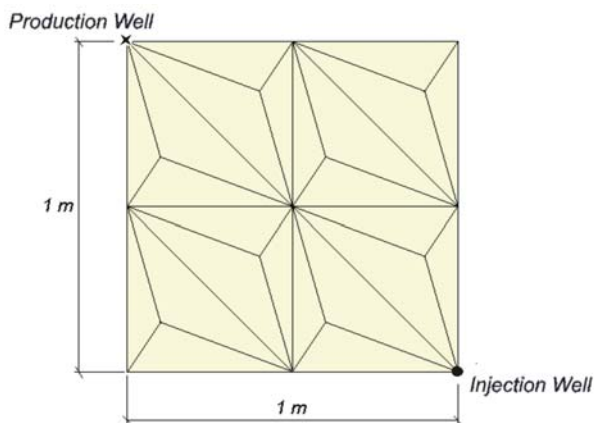
Figure 11 – Grid for the Problem 5

The data utilized in this test problem are listed in Tab. 1, except for the water flow-rate at the injection well that was changed to 0.1 m³/d in this problem.

Figure 12 shows the different water-cut curves obtained by different methods. Although the differences verified between these curves are not so evident, the water-saturation contour, in contrast, is very different in both methods, as we can see in Fig. 13. Despite the fact that the grid used is not really symmetric (c.f. Fig. 11), the CVFEM-S results

show exaggerate asymmetry, Fig. 13*a*, differently of the results obtained by the other method, Fig. 13*b*. Therefore, once again the CVFEM-M yields more physically coherent results.
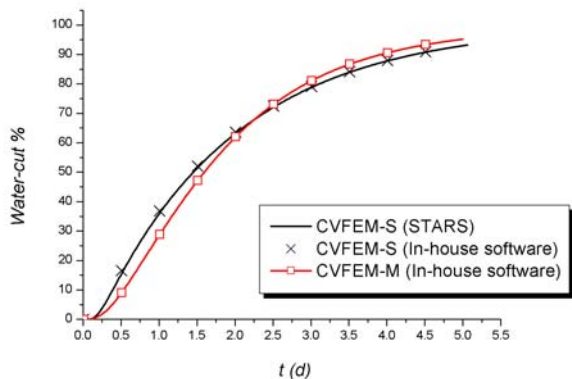
Figure 12 – Comparison of water-cut curves for Problem 5

| $t = 1.25$d | $t = 2.09$ d |
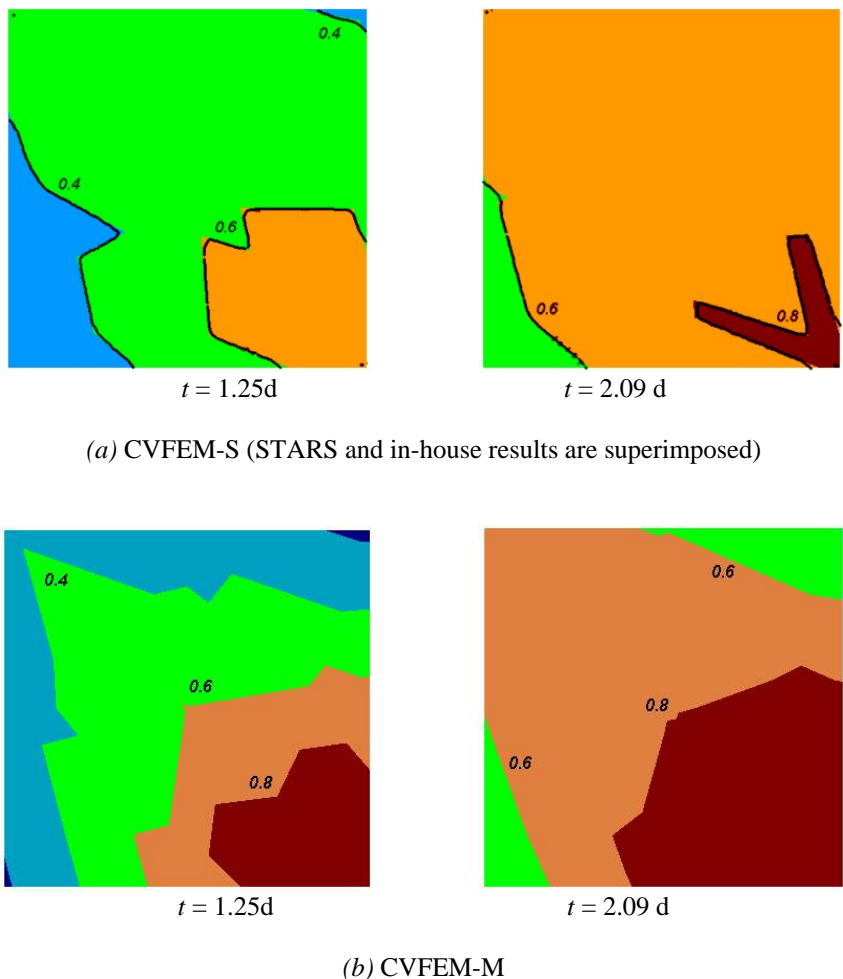
(a) CVFEM-S (STARS and in-house results are superimposed)

| $t = 1.25$d | $t = 2.09$ d |

(b) CVFEM-M

Figure 13 – Water-saturation contour at different simulation times, obtained from: *(a)* CVFEM-S, and *(b)* CVFEM-M

3. Conclusions

This work exemplified, with several key problems, the theoretical issues presented in the companion paper. Initially, it was demonstrated that the concept of transmissibility has been used in a misleading way, leading to a conclusion that obtuse triangles should be avoided in grid generation. In fact the negative coefficients that appear are not transmissibility and the results are physically consistent. The effects of these negative coefficients on the convergence of linear solvers need to be further investigated.

Three different schemes of evaluating mobilities at the control-volume interfaces were presented. It was shown that according to the scheme chosen, the water saturation can result in negative values. The scheme proposed with the CVFEM-M, on the other hand, assures that the mobilities used are those located on the upstream direction.

Finally, one can conclude that the procedure of obtaining the multiphase equations introducing the mobility to the flow terms in the single-phase discretized equations is not correct for triangular grids, where the flow can be correctly calculated only using three nodal values. This procedure results in a scheme that has several difficulties in practical problems, like loss of flexibility and greater grid orientation effect. Otherwise, if the equations are correctly deduced, the resulting discretizing equations are the same as those obtained by the CVFEM-M, which are closely related to the physical process.

4. Acknowledgements

5. References

Bajor, O. and Cormack, D. E., 1989. "A New Method for Characterizing the Grid Orientation Phenomenon", SPE paper 19353, Society of Petroleum Engineering.

Baliga, B. R. and Patankar, S. V., 1983. "A Control Volume Finite-Element Method for Two-Dimensional Fluid Flow and Heat Transfer", Numerical Heat Transfer, vol. 6, pp. 245-261.

Cordazzo, J., Maliska, C. R., Silva, A. F. C., and Hurtado, F. S. V., 2004. "The Negative Transmissibility Issue When Using CVFEM in Petroleum Reservoir Simulation -- 1. Theory", Proceedings of the 10o Brazilian Congress of Thermal Sciences and Engineering -- ENCIT 2004, Braz. Soc. of Mechanical Sciences and Engineering -- ABCM, Rio de Janeiro, Brazil, Nov. 29 -- Dec. 03.

Fung, L. S., Hiebert, A. D. and Nghiem, L., 1991. "Reservoir Simulation with a Control-Volume Finite-Element Method", SPE paper 21224 presented at the 11th SPE Symposium on Reservoir Simulation, Anaheim, California, February 17-20.

Palagi, C., 1992. "Generation and Application of Voronoi Grid to Model Flow in Heterogeneous Reservoir", Doctor Thesis, Stanford University, California.

Schneider, G. E. and Zedan, M., 1983. "Control-Volume-Based Finite Element Formulation of the Heat Conduction Equation, in Spacecraft Thermal Control", Design, and Operation, Prog. Astronaut. Aeronaut., vol. 86, pp. 305-327.

Shin, D. and Merchant, A. R., 1993. "Higher-Order Flux Update Function Method for Reduction of Numerical Dispersion and Grid Orientation Effect in Reservoir Simulation", SPE paper 25600 presented at the SPE Middle East Oil Technical Conference & Exhibition, Bahrain, 3-6 April.

Sonier, F., Lehuen, P. and Nabil, R., 1993. "Full-Field Gas Storage Simulation Using a Control-Volume Finite Model", SPE paper 26655 presented at the 68th Annual Technical Conference and Exhibition of the Society of Petroleum Engineers, Houston, Texas, 3-6 October.

Stars User's Guide, 2002. "Advanced Process and thermal Reservoir Simulator", by Computer Modelling Group Ltd., Alberta Canadá.

Todd, M. R., O´Dell, P. M., and Hirasaki, G. J., 1972. "Methods for Increased Accuracy in Numerical Reservoir Simulators", Soc. Pet. Eng. J., Dec., 515-530.

Yanosik, J. L. and Mccracken, T. A., 1979. "A Nine-Point Finite-Difference Reservoir Simulator for Realistic Prediction of Adverse Mobility Ratio Displacements", SPEJ, Aug., 253-262; Trans., AIME, 267.